



22nd IAHR International Symposium on Ice
Singapore, August 11 to 15, 2014

Preliminary Results From Two Years of Ice Stress Measurements in a Small Reservoir

Chris Petrich^{1*}, Irina Sæther¹, Lennart Fransson², Bjørnar Sand¹, and Bård Arntsen¹

1. Norut Narvik, Narvik, Norway

2. Luleå University of Technology, Luleå, Sweden

** christian.petrich@norut.no*

Design standards for hydropower dams and other reservoir dams require ice loads to be considered. Ice stress measurements were performed in a small reservoir near Narvik, Norway in 2012/13 and 2013/14 in an effort to identify the signature of thermal ice stresses and distinguish them from mechanical stresses due, for example, to bending. Stresses observed could be related to temperature changes in the ice and indicated the combined action of thermal expansion and secondary creep. Both compressive and, to a limited extent, tensile stresses were recorded during warming and cooling periods, respectively. Stresses tended to be lowest at the periphery of the dam in 2012/13. Several events of mechanical loading were observed in Season 2013/14. It is concluded that current knowledge of ice loads in small reservoirs is limited and that several seasons of data are required to obtain an overview of processes, modes and magnitudes of loads.

1. Introduction

Norway has a large number of dams of increasing age. They represent a considerable value in terms of fixed capital assets and future generation profits. The consequences of a dam failure could be significant, resulting in economic and environmental damage, and safety is therefore given highest priority. A new regulation to the Water Resources Act (Vannressursloven) that addresses safety at hydropower plants (damsikkerhetsforskriften) was implemented in 2010. The new guidelines and design recommendations also include new considerations regarding ice pressure/loads on dams and other types of hydro-electrical structures (NVE, 2003). The new regulations for dam safety cause a need for upgrading and strengthening of existing dams and infrastructure. This is especially the case for a large number of smaller concrete dams that will not be able to meet the requirements specified in the new guidelines. Small dams (less than 15 m height) account for approximately 90% of the dams in Norway. For the time being, design standards are based on empirical measurements as current understanding of the magnitude of ice loads is still limited (Timco et al., 1996; Comfort et al., 2003; Gebre et al., 2013). According to the new guidelines, thermal ice loads are assumed to be line loads between 100 and 150 kN/m near the top of the dam. However, the basis for this assessment is limited. Field measurements of ice forces on dams have suggested that the ice load vary significantly depending on where the dam is located, climate and sudden temperature changes (Gebre et al., 2013). The maximum ice load value determined in Norway was 135 kN/m during only one season of measurements at Silvann dam in the Northern part of Norway (Hoseth and Fransson, 1999). Increasing efforts to understand ice loads on dams has been called for (Gebre et al., 2013). A more profound understanding of the mechanisms involved in ice–structure interactions may lead to the development of more cost efficient strategies for reducing the actual ice-load on the dam. This is especially interesting in designing small dams for small scale hydropower plants.

2. Methods

Measurements were performed at Taraldsvikfossen Reservoir in Narvik, 68.4405° N, 17.471° E, 212 m above sea level (Figure 1a). The reservoir has a surface area of approximately 1000 m², is not in service and maintained as a back-up for drinking water supply. It is confined by a straight-sided concrete dam, 6 m high. A fraction of the waters of a creek, Taraldsvikelva, enters the reservoir during most of the year, keeping the water in the reservoir at the level of the spill way. The water level is 0.5 m below the dam surface, except during surges. As the creek freezes in winter, flow in and out of the reservoir ceases or reduces significantly. Flow rates of the creek are recorded by the Norwegian Water Resources and Energy Directorate (NVE) approximately 700 m upstream. There, flow rates reach typically 0.5 m³/s in May/June and may exceed 1 m³/s briefly. However, winter flow rates are typically as low as 0.005 m³/s.

Environmental conditions were recorded in addition to stresses in the ice. A Vaisala WXT 520 weather transmitter and an Apogee SP212 amplified pyranometer were mounted at the SE corner of a maintenance hut at the center of the dam, 3.5 m above the dam surface. A downward-facing Campbell Scientific SR50A acoustic ranger overlooked the reservoir to register changes in water level, ice level or snow depth. From season 2013/14, a Campbell Scientific CS456 water pressure transducer was mounted approximately 1.5 m below the water level. A 3 m-long string with Maxim DS18B20 digital temperature sensors spaced 0.1 m was frozen into the ice near the pressure cells (Station 5 and F' in 2012/13 and 2013/14, respectively). The probe was deployed

such that the upper 0.6 m reached through snow and into air and 2.4 m reached through ice and into water. One and two UM562 automated cameras overlooked part of the reservoir and recorded photos every 30 minutes during season 2012/13 and 2013/14, respectively.

Ice stresses were recorded with custom-modified oil-filled GeoKon 4850 pressure cells (similar cells were used by Taras et al. (2011)). The cells register normal pressure and consisted of two rectangular steel plates (100 mm x 200 mm) welded together around the periphery with a de-aired fluid occupying the space between the plates. A short tube connected the cell to a vibrating wire pressure transducer. The cells were custom built to a design pressure range of 1 MPa, the stress tube was removed, and the pressure transducer was connected in the plane of the plates. Pressure cells were mounted on steel tape at 0.15 m vertical intervals (0.25 m at Station W in 2012/13). Cells fixed to the dam in season 2013/14 were mounted on a frame (Figure 1b) with the center of the top-most cell 0.1 m below the water line. Cells located in the ice 1 to 2 m in front of the dam and elsewhere in the reservoir were deployed in slots cut with a chain saw (Figure 1c) with the center of the top-most cell 0.2 m below the ice surface at the time of deployment. Only approximately half of the measurement stations had 3 pressure cells stacked vertically. The remaining stations had 1 pressure cell at the vertical position of the upper-most cell (Table 1). With the exception of frame-mounted cells of group I, cells were deployed in a slot cut into the ice after an ice cover had formed. After installation, the slot was filled with water and left to refreeze.

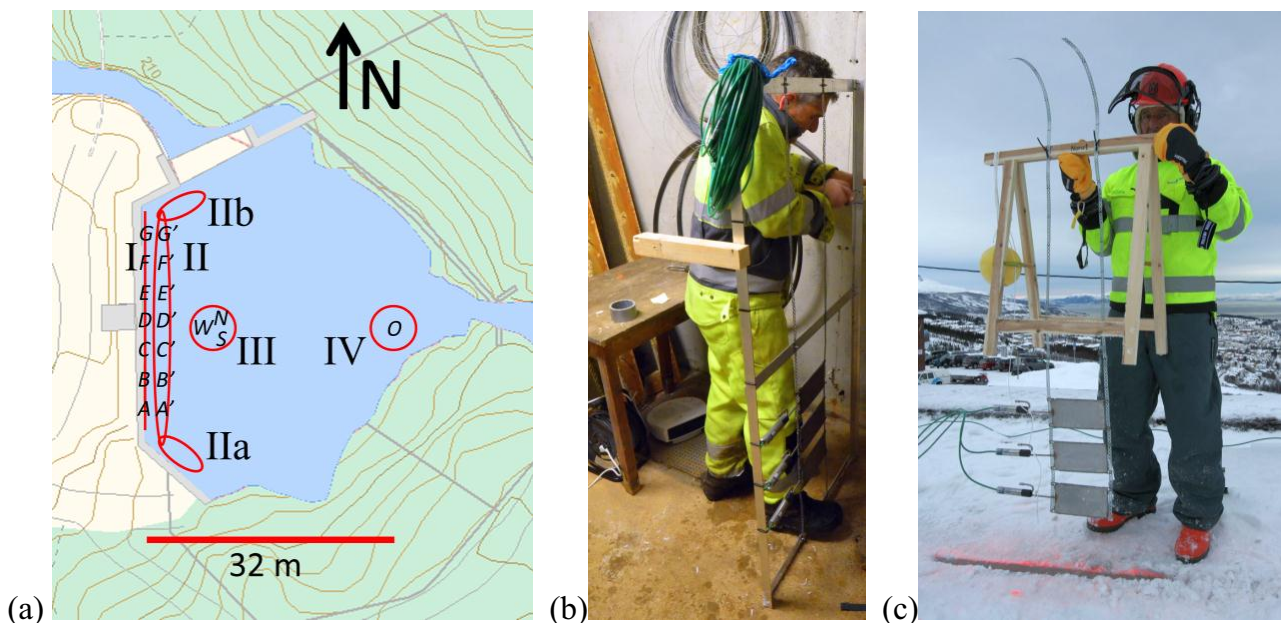


Figure 1. (a) Schematic of the arrangement of pressure cells in the reservoir. Roman numerals are group numbers of Table 1. 2014 Station names are given in italics. Map courtesy NVE. (b) Frames with pressure cells mounted directly at the dam (season 2013/14). The center of the upper-most cell was installed 0.1 m below the water level. (c) Pressure cells installed in front of the dam and elsewhere in the reservoir (seasons 2012/13 and 2013/14). The center of the upper-most cell was installed 0.2 m below the ice surface.

All instruments were connected to a CR1000 data logger installed inside the maintenance hut. Power was provided by 230 V mains and a 12 V backup battery. Logger and data were accessible remotely through a GPRS link.

With the exception of Stations N and S, all pressure cells were mounted parallel to the dam, i.e. registering stresses in direction normal to the dam. In season 2012/13, Stations 1 to 6 were placed in front of the dam into the ice (Figure 1a). Stations 1 and 6 (i.e., groups IIa and IIb, respectively) were located on the flanks rather than the main section of the dam. In season 2013/14, Stations A to G were placed onto the main section of the dam (group I), Stations A' to G' were placed at the corresponding positions in front of the dam (group II), and Station O was placed 31 m from dam at the center of the main section, i.e. essentially at the opposite side of the reservoir (group IV). Stations N, S, and W were installed approximately 10 m in front of the dam and rotated 60° with respect to each other in an equilateral triangle with 2 m side length (group III), allowing principal stresses to be calculated easily (Holister, 1967).

Table 1. Position of pressure cells. Location of groups is illustrated in Figure 1a. Lateral position is measured from the center of dam (i.e., 0.8 m South of the center of the maintenance hut), except groups IIa and IIb where it is measured from the corner of the dam. Negative numbers are to the South. Normal position is measured perpendicular to the dam face.

2012/13							
	1	2	3	4	5	6	N,S,W
Group	IIa	II	II	II	II	IIb	III
Cells	1	3	1	3	3	1	1,1,3
Lateral (m)	-4.2	-10.3	-5.9	-0.3	9.4	6.4	0.7
Normal (m)	1.2	1.1	1.1	1.1	1.4	1.8	7.8

2013/14							
	A	B	C	D	E	F	G
Group	I	I	I	I	I	I	I
Cells	1	3	1	3	1	3	1
Lateral (m)	-12	-7.5	-3.5	0	3.5	7.5	11.5
Normal (m)	0.01	0.01	0.01	0.01	0.01	0.01	0.01

	A'	B'	C'	D'	E'	F'	G'	N,S,W	O
Group	II	II	II	II	II	II	II	III	IV
Cells	1	3	1	3	1	3	1	1,1,3	1
Lateral (m)	-11.9	-7.5	-3.3	0	3.5	7.6	11.3	0.7	0
Normal (m)	1.9	1.9	1.9	1.9	1.9	1.9	1.9	10.5	31

In season 2012/13, the date of onset of ice formation is unknown. However, the ice cover was stable by 5 Dec 2012 and measured to be 0.5 to 0.6 m thick on 12 Dec. All pressure cells were installed on 12 Feb 2013. Ice thickness at Stations 1 to 6 was 0.75 m with 0.21 m freeboard and snow depth between 0.05 (Station 5) and 0.2 to 0.32 m (all other stations). Ice thickness at Stations W, N, and S was 1.0 m with 0.09 m freeboard and 0.26 m snow cover. Air temperatures were consistently above 0 °C from 14 Apr on. Pressure cells started to melt out and lost good

contact with the ice at the end of April and were melted out and easily removed from the ice on 14 May 2013. The ice cover broke up from 18 to 22 May 2013.

In season 2013/14, ice formation started during a cold spell on 17 Oct 2013 (air temperature $-8\text{ }^{\circ}\text{C}$). Ice was removed at the dam and pressure cells of group I were installed on 23 Oct. Ice thickness was about 0.1 m. Pressure cells of groups II, III, and IV were installed on 11 Feb 2013. Ice thickness at group II was 0.78 m with 0.28 m freeboard and no snow. Ice thickness and freeboard were 0.67 and 0.05 m and 0.80 and 0.14 m at groups III and IV, respectively. Ice began to weaken and melt and ice around the pressure cells started to melt from mid-April. The ice cover broke up from 24 to 29 May 2014.

3. Results

The time lapse cameras installed at the reservoir resulted in a valuable, qualitative record of ice formation and decay, surface melt, surface condition (bare ice, snow, slush), snow fall and drift, surface flooding, and bending of the ice cover. By comparing time lapse images, we found that Season 2013/14 was more dynamically and thermodynamically active than 2012/13. It appears as though the water level and pressure increased in the reservoir occasionally due to inflow from the creek, resulting in upward movement at the center or bending of the ice cover (in the following collectively referred to as “bending”). The overpressure was relieved within hours or less than one week, usually accompanied by partial flooding of the ice cover to various extent (e.g., Figure 2b). The last evidence of visible changes in ice level had been recorded on 11 Jan 2013 and 4 Feb 2014, respectively. Later in the season a small but continuous stream of water was observed to run down the spill way from beneath the ice cover, thereby effectively preventing pressure build-up in the reservoir. In season 2012/13, water was flowing continuously since 27 Feb, which was consistent with the break-down of stratification and onset of mixing recorded by the temperature probe. In season 2013/14, stratification broke down as early as 12 Dec. In season 2013/14, two bending events had occurred before early Dec. From early Dec until deployment of pressure cells in mid Feb, two and four bending events had occurred in seasons 2012/13 and 2013/14, respectively. Since installation of the sensors bending had not been observed but small degrees of surface flooding occurred in the vicinity of cracks on 8 and 20 Mar 2013 (associated with air temperatures below $-10\text{ }^{\circ}\text{C}$). In 2014, the ice surface was partially flooded by water from the creek from 10 to 12 Mar (air temperatures above $0\text{ }^{\circ}\text{C}$) and 17 to 18 Mar (air temperatures below $-10\text{ }^{\circ}\text{C}$). Based on preliminary data from NVE, Taraldsvikelva experienced winter flow rates in winter season 2013/14 significantly higher than during the previous 5 winters. Surface melt (slushy snow or ponds in the presence of air temperatures above $0\text{ }^{\circ}\text{C}$) occurred after the installation of sensors in mid-Feb until mid-Apr on one and five occasions in seasons 2012/13 and 2013/14, respectively (Figure 2a). Snow cover was significant in Season 2012/13 with 0.2 to 0.3 m common from mid-Jan, while comparatively insignificant in Season 2013/14, mostly due to less snow fall in general and partly due to more frequent flooding and surface melt. $0\text{ }^{\circ}\text{C}$ -based Freezing Degree Days were 900 and 600 $^{\circ}\text{C}$ days in season 2012/13 and 2013/14, respectively.

Observations early in the season showed that, in both seasons, dry cracks formed 1 to 5 cm from the dam face, around 1 to 2 m from the dam, and at other distances from the dam. Due to occasional warm spells and flooding, the cracks may or may not have refrozen and were mostly hidden by a solid ice cover in mid-Feb. Cracks are important features for the ice loads in lakes

(Metge, 1976; Comfort et al., 2003) and we found that the crack passing 2 m off the NW and SW corners of the reservoir is the likely source of flooding near the corners (e.g., during cold spells).

Ice conditions in Season 2012/13 were nearly ideal for the measurement of thermally induced stresses. Pressure cells were installed in the ice cover in mid-Feb and froze in, recording high initial pressures due to volume expansion during freezing of surrounding water that slowly decayed as a result of creep (e.g. Cox, 1984; Fransson, 1988). Pressure readings returned to their original zero-reading during a warm spell from 24 Feb until 1 Mar. However, during the subsequent temperature decrease, none of the cells showed signs of freeze-in artifacts. This resulted in approximately 6 weeks of quality data of thermal stresses until the ice finally decayed starting 14 Apr. In Season 2013/14, the only period dominated by thermal loads was from 14 Feb to 14 Mar, a time where stress around the pressure cells installed in mid-Feb had potentially not equilibrated after freeze-in. Occasional signs of thermal load were seen until early April.

In 2012/13, stresses were found to be highest close to the center of the dam, decreasing toward the flanks. Stresses in season 2013/14 were distributed seemingly unsystematically often, but not always. Vertical profiles of normal stress onto the dam were found to be generally not linear. This could have been related to cracks similar to observations of Comfort et al. (2003).

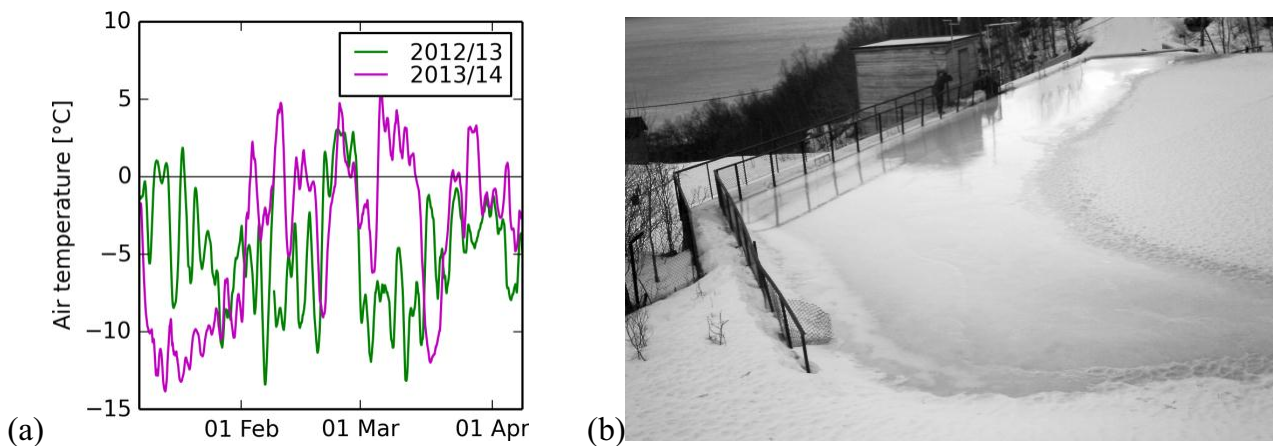


Figure 2. (a) Air temperature record from Jan to Apr 2013 and 2014. (b) Photo overlooking dam and part of the reservoir from the South on 18 Jan 2014 following flooding at the perimeter.

Figure 3 gives an overview of data of the top-most cells in groups I and II at different times. Positive pressure readings of the cells indicate that the ice was in compression. While no complete discussion of data can be given here, examples of different types of observations made shall be given. Station G is not shown because readings stayed close to 0 throughout the season for a reason to be determined. Stresses at the dam most likely due to mechanical forces in Season 2013/14 are shown in Figure 3a. The peak around 17 Jan 2014 ends as the surface started to flood and the ice cover started to move upward at the center of the reservoir. This may indicate that increasing water pressure in the reservoir resulted in opening of cracks. The peak starting on 18 Jan 2014 is associated with downward-movement of the ice and sounds reminiscent of collapsing ice layers (Figure 2b). Very high pressures had been recorded at the center of the dam, reaching 0.6 MPa. Figure 3b shows a period of presumably thermal stresses in group I during 2013/14 with peaks corresponding to periods of temperature rise (Figure 2a). Possibly most

remarkable is the record of negative pressure, i.e., tension in the ice around 21 Feb. Apparently, Stations A and F had ice connected to cells to pressures as low as -0.2 MPa. On 25 Feb, with the highest pressure recorded at Station A (0.4 MPa) and the lowest pressure at D, stress distribution deviated remarkably from the general “highest at the center” assumption. Figure 3c illustrates the challenge of gradual pressure relaxation after initial freeze-in of sensors in group II (Cox, 1984; Fransson, 1988). While stress signals appear at the same time as measured at the dam (Figure 3b), the zero-point is ill-defined and we may only be able to make statements regarding change on stress over relatively short periods of time. Also, based on earlier reports (e.g. Taras et al. (2011)), one may have expected to see stronger correspondence between readings of sensors in groups I and II. However, the sensors in group II (Figure 3c) are higher up in the ice than those of group I (Figure 3b) so that peaks around 25 Feb and 6 Mar could not develop because ice around the sensors started to melt (Figure 3c). Figure 3d shows a period of thermal stresses in group II during Season 2012/13. As described above, there are no signs of freeze-in artifacts at the end of the warm-spell on 1 Mar. Instead, stresses seem to be related to rate of ice temperature change from the start. We assume that stresses are predominantly thermal because it appears they can be described over periods of weeks with a simple model modified after Bergdahl, using only the rate of change of ice temperature and location-dependent coefficients (Cox, 1984; Fransson, 1988). Recorded pressures ranged from 0.2 MPa in compression to -0.1 MPa in tension.

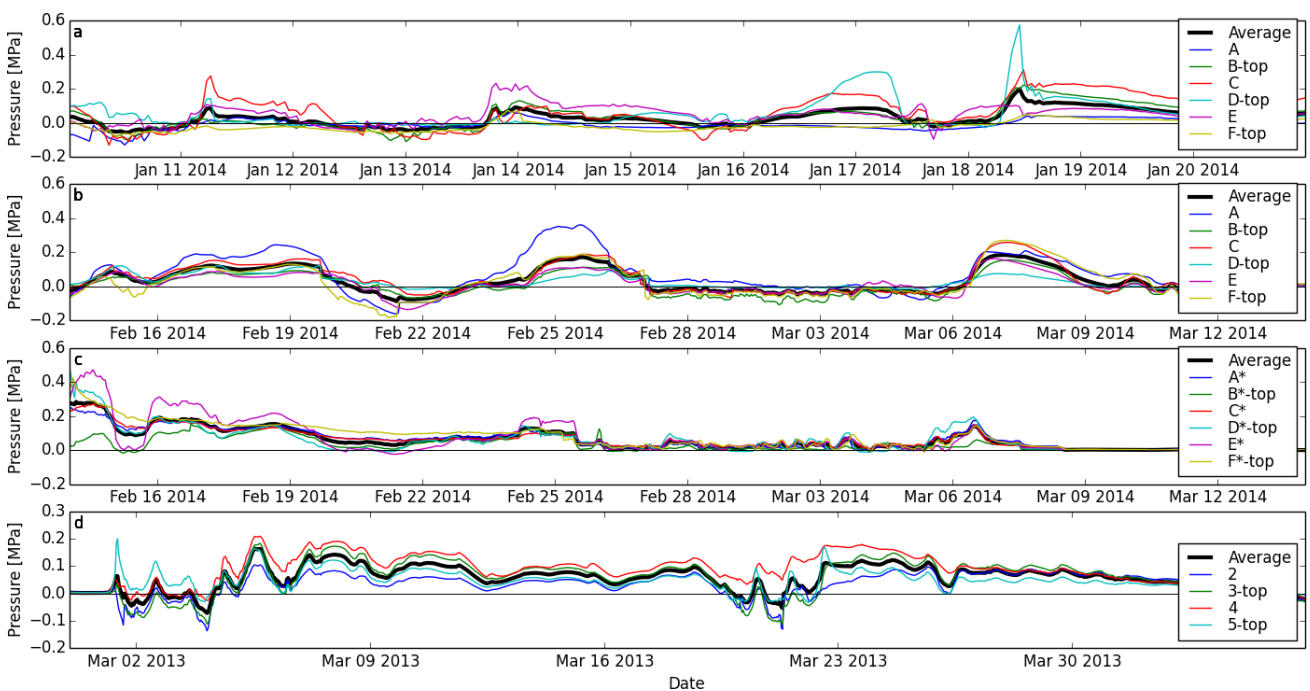


Figure 3. Examples of pressure cell data of the top-most cells at the respective stations. (a) 2014 group I, (b) 2014 group I, (c) 2014 group II, same time as (b), (d) 2013 group II. Averages are calculated from the data shown. Note the different scales.

4. Conclusions

Ice stresses were measured in two consecutive seasons in a small reservoir. Pressure cells were frozen into the ice and recorded both compression and, to a limited degree, tension. The chosen symmetric configuration included redundancy that allows us to test for common hypotheses rather than limiting us to extrapolating loads.

The measurements illustrate that a “typical” stress field in an ice-covered reservoir cannot always be inferred from a single season of measurement. Data show that stresses due to either thermal expansion or mechanical events may be dominating. While detailed evaluation of the data is ongoing, our preliminary conclusions are consistent with the assessment of Gebre et al. (2013), i.e. that current understanding of ice loads is deficient. Actual ice loads onto dams may not be trivial to measure or relate to their causes. In particular, uncertainty is introduced by the type of attachment of ice to the boundaries, presence of cracks, and occurrence of bending. However, our evidence of systematic distribution of thermal stresses in the ice cover promises potential for numerical modeling of thermal stresses none-the-less. Detailed evaluation of the data record is ongoing.

Acknowledgments

This work was funded by NVE, Statkraft, and the Norwegian Research Council project number 195153 (ColdTech) with industry partners. The excellent support of Tore Pettersen and Martin Arntsen in instrument preparation, deployment, and recovery is gratefully acknowledged. Narvik Kommune kindly provided access to the Taraldsvikfossen Reservoir.

References

- Comfort, G., Y. Gong, S. Singh, and R. Abdelnour, 2003. Static ice loads on dams. *Canadian Journal of Civil Engineering*, 30, 42–68.
- Cox, G. F. N., 1984. A preliminary investigation of thermal ice pressures. *Cold Regions Science and Technology*, 9, 221–229.
- Fransson, L., 1988. Thermal ice pressure on structures in ice covers. Doctoral Thesis, Luleå University of Technology, Sweden, 161pp.
- Gebre, S., Alfredsen, K., Lia, L., Stickler, M., and Tesaker, E., 2013. Review of ice effects on hydropower systems. *Journal of Cold Regions Engineering*, 27(4), 196–222.
- Holister, G. S. (1967), *Experimental Stress Analysis*. Cambridge Engineering Series, Cambridge University Press, Bentley House, London, UK, 321pp.
- Hoseth, K.A. and L. Fransson, 1999. Istrykk på dammer. Måleprogram dam Silvann, vinter 98-99. Report nr 21., Norges vassdrags- og energidirektorat, Oslo, 34 pp.
- Metge, M., 1976. Thermal cracks in lake ice. Ph.D. thesis, Queen’s University, Kingston, Ontario, Canada, 204pp.
- NVE, 2003. Retningslinje for laster og dimensjonering til §§ 4-1 og 4-2 i forskrift om sikkerhet og tilsyn med vassdragsanlegg Norges vassdrags- og energidirektorat. Norges vassdrags- og energidirektorat, Oslo. 25pp.
- Taras, A., A. Côté, G. Comfort, L. Thériault, and B. Morse, 2011. Measurements of ice thrust at Arnprior and Barrett Chute dams. In *Proceedings of the 16th Workshop on the Hydraulics of Ice Covered Rivers*, Winnipeg, MB, Canada, 18–22 September 2011, 317–328.
- Timco, G.W., D. A. Watson, G. A. Comfort, and R. Abdelnour, 1996. A comparison of methods for predicting thermally-induced ice loads. *Proceedings of the 13th IAHR Symposium on Ice*, Beijing, China, vol. 1, 241-248.